PHYSICAL REVIEW B **77**, 100405(R) (2008)

Low-temperature phase boundary of dilute-lattice spin glasses

Stefan Boettcher and Emiliano Marchetti
Physics Department, Emory University, Atlanta, Georgia 30322, USA
(Received 3 March 2008; published 27 March 2008)

The thermal-to-percolative crossover exponent ϕ, well known for ferromagnetic systems, is studied extensively for Edwards–Anderson spin glasses. The scaling of defect energies are determined at the bond percolation threshold p_c using an improved reduction algorithm. Simulations extend to system sizes above $N=10^8$ in dimensions $d=2,\ldots,7$. The results can be related to the behavior of the transition temperature $T_g \sim (p-p_c)^{\phi}$ between the paramagnetic and the glassy regime for $p \searrow p_c$. In three dimensions, where our simulations predict $\phi=1.127(5)$, this scaling form for T_g provides a rare experimental test of predictions arising from the equilibrium theory of low-temperature spin glasses. For dimensions near and above the upper critical dimension, the results provide a challenge to reconcile mean-field theory with finite-dimensional properties.

DOI: 10.1103/PhysRevB.77.100405 PACS number(s): 75.10.Nr, 02.60.Pn, 64.70.P−, 64.70.Q−

The exploration of low-temperature properties of disordered systems remains an important and challenging problem.[1,2] The paradigmatic model for such phenomena is the Edwards–Anderson (EA) spin glass,[3]

$$H = -\sum_{\langle i,j\rangle} J_{i,j} x_i x_j \quad (x_i = \pm 1). \tag{1}$$

Disorder effects arise via quenched random bonds, $J_{i,j}$, mixing ferro- and antiferromagnetic couplings between nearest-neighbor spins, which lead to conflicting constraints and frustrated variables. It is believed that an understanding of static and dynamic features of EA may aid a description of the unifying principles expressed in glassy materials.[3] Most insights into finite-dimensional systems have been gained through computational approaches that elucidate low-T properties.[4–6]

Here, we extract the response induced through defect interfaces[7,8] at $T=0$, created by fixing the spins along the two faces of the open boundary in one direction. Ground state energies E_0 and E_0' of an instance of size $N=L^d$ are determined, which differ by reversing all spins on *one* of the faces. The distribution $P(\Delta E)$ of interface energies $\Delta E = E_0' - E_0$ created by this perturbation of scale L on the boundary is obtained. The typical energy scale, represented by the deviation $\sigma(\Delta E)$, grows as

$$\sigma(\Delta E) \sim L^{y}. \tag{2}$$

This relation defines[3,7,8] the stiffness exponent y characterizing the defect energy, a fundamental quantity assessing low-temperature fluctuations: a positive value of y, as found[9] in EA for $d > d_l \approx 5/2$, denotes the increase in the energetic cost accompanying a growing number of variables perturbed from their position in the ground state (i.e., "stiffness"). The rise in strain for stronger disturbances signals the presence of an ordered state. In turn, for systems with $y \leqslant 0$, such order is destabilized by fluctuations that spread unimpeded.

Instead of determining the interface scaling on a compact lattice structure, we will focus here on the interface energy $\sigma(\Delta E)$ on a *bond-diluted* lattice, particularly at the percolation threshold p_c (see Fig. 1). Due to the tenuous fractal nature of the percolating cluster at p_c, no long-range order can be sustained, and[10]

$$\sigma(\Delta E)_{L,p_c} \sim L^{y_P} \quad \text{with } y_P \leqslant 0, \tag{3}$$

i.e., defects possess a vanishing interface energy. Interest in the exponent y_P stems from its relation to the "thermal-percolative crossover exponent" ϕ defined via[10]

$$T_g(p) \sim (p-p_c)^{\phi} \quad \text{with } \phi = -\nu y_P, \tag{4}$$

where ν is the correlation-length exponent associated with lattice percolation,[11,12] $\xi \sim (p-p_c)^{-\nu}$. Of particular experimental interest is the result for $d=3$, $y_P=-1.289(6)$, predicting $\phi=1.127(5)$, with $\nu=0.874\,36(46)$.[13] All results for $d=2,\ldots,7$ are listed in Table I.

The exponent ϕ was studied intensely numerically, theoretically, and experimentally[12,16–22] for ferromagnetic systems some 30 years ago and was just recently discussed for quantum spins.[23] However, aside from its initial treatment in Ref. 10, there are no other investigations on spin glasses. This is even more surprising since this exponent provides a nontrivial, experimentally testable prediction derived from scaling arguments of the equilibrium theory at low temperatures. Such tests are few as disordered materials by their very nature fall out of equilibrium when entering the glassy state. The phase boundary itself provides the perfect object for such a study: It can be approached by theory from below and by experiments from above where equilibration is possible.

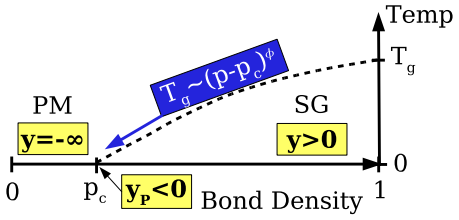

FIG. 1. (Color online) Phase diagram for bond-diluted spin glasses ($d > d_l$). In the spin glass phase (SG) for $T < T_g$ and $p > p_c$, y in Eq. (2) is >0, while $y=y_P<0$ in Eq. (3) at $p=p_c$ and $T=T_g=0$. In the paramagnetic phase (PM) for $p < p_c$, defects decay exponentially for all T. The exponent ϕ in Eq. (4) describes the boundary $T_g(p)$ for $p \searrow p_c$.

TABLE I. List of the parameters used and exponents found in our simulations for $d=2,\ldots,7$. $L_{\max}$ denotes the largest lattice size considered. We have used the bond-percolation thresholds p_c from Ref. 14 for $d=3$ and Ref. 15 for $d\geqslant 4$. The correlation-length exponents ν for percolation are from Ref. 13 in $d=3$ and from Ref. 11 for $d\geqslant 4$, where $\nu=1/2$ is exact above the upper critical dimension, $d\geqslant 6$.

d	p_c	ν	y_P	$\phi=-\nu y_P$	$L_{\max}$
2	1/2	4/3	−0.993(3)	1.323(4)	1000
3	0.2488126	0.87436(46)	−1.289(6)	1.127(5)	300
4	0.1601314	0.70(3)	−1.574(6)	1.1(1)	100
5	0.118172	0.571(3)	−1.84(2)	1.05(2)	35
6	0.0942019	0.5	−2.01(4)	1.00(2)	25
7	0.0786752	0.5	−2.28(6)	1.14(3)	15

There is reason to believe that the phase boundary in Eq. (4) and Fig. 1 is experimentally accessible for certain materials. Reference 24 already provided highly accurate results for the freezing temperature T_M as a function of dilution x for a doped crystalline glass, $(La_{1-x}Gd_x)_{80}Au_{20}$, proposing a linear dependence, $T_M\sim x$. The tabulated data are equally well fitted by Eq. (4) in that regime. Reference 25 determined a phase diagram for $(Fe_xNi_{1-x})_{75}P_{16}B_6Al_4$, an amorphous alloy, for a wide range of temperatures T and site concentrations x but did not discuss its near-linear behavior at low x. A similar phase diagram for the insulator $CdCr_{2x}In_{2(1-x)}S_4$ can be found in Fig. 1.1a of Ref. 26. Experiments dedicated to the limit $x\searrow x_c$ should provide results of sufficient accuracy to test our prediction for ϕ.

A match of computational prediction and experiment would lend credibility to the EA model and its simplifying assumptions, such as universality with respect to the details of the bond distribution $P(J)$, an issue recently revisited by Ref. 27. Our simulations, conducted here for Gaussian bonds, can be repeated for any $P(J)$ of zero mean and unit variance but would significantly increase computational cost. Simply to demonstrate that theoretically such universality exists, we have repeated our simulations with a Lorentzian bond distribution argued for by Ref. 28 and with power-law-distributed bonds $P(J)\propto|J|^{\alpha-1}$ for $|J|\geqslant 1$ at $\alpha=-1/2$. This comparison, presented below in Fig. 3, clearly shows reproducibility for a wide class of $P(J)$. Reference 10 also considered power-law distributions, but for $\alpha>0$ and $|J|<1$, to point out that the response to perturbations is, in principle, nonuniversal at p_c: Without a long-range order, it is $y\leqslant 0$ in Eq. (2) and energy scales do *not* divere. Then, y (and ϕ) becomes dependent on the details of $P(J)$ near $J=0$, and Ref. 10 finds an interesting change in behavior for $\alpha<\alpha_c\approx 0.75$. Such a diverging bond distribution results from integrating the RKKY couplings (see Ref. 3) over many weak bonds in its far-distance tail. In realistic materials, such bonds are screened out (see, for instance, Ref. 24), and $P(J)$ is bounded, justifying the use of Gaussian bonds.

Following the discussion in Refs. 10 and 29, for diluted lattices at $p\to p_c$, we have to generalize the scaling relation for the defect energy $\sigma(\Delta E)$ in Eq. (2) to

$$\sigma(\Delta E)_{L,p}\sim \mathcal{Y}(p)L^y f[L/\xi(p)]. \tag{5}$$

Here, $\mathcal{Y}\sim(p-p_c)^t\sim\xi^{-t/\nu}$ is the surface tension and $\xi(p)\sim(p-p_c)^{-\nu}$ is the correlation length for percolation. The scaling function f is defined to be constant for $L\gg\xi(p)\gg 1$, where percolation (and, hence, ξ) plays no role and we regain Eq. (2) for $p>p_c$.

For $\xi\gg L\gg 1$, Eq. (5) requires $f(x)\sim x^\mu$ for $x\to 0$ to satisfy $\sigma\to 0$ with some power of L, which is needed to cancel the ξ dependence at $p=p_c$. Thus, $\mu=-t/\nu$, and if we define $y_P=y+\mu=y-t/\nu$ to mark the L dependence of σ at $p=p_c$ as in Eq. (3), we get $t=\nu(y-y_P)$. Finally, at the crossover $\xi\sim L$, where the range L of the excitations $\sigma(\Delta E)$ reaches the percolation length beyond which spin glass order ensues, Eq. (5) yields with ϕ from Eq. (4),

$$\sigma(\Delta E)_{\xi(p),p}\sim(p-p_c)^t\xi(p)^y f(1)\sim(p-p_c)^\phi. \tag{6}$$

Associating a temperature with this crossover by $\sigma(\Delta E)_{\xi(p),p}\sim T_g$ (for $T>T_g$, thermal fluctuation destroy order) leads to Eq. (4), relating p and T_g.

In our simulations, we have used the method of bond reductions described previously.[30–32] A set of rules is defined and applied recursively to trace out spins, assuming that $T=0$. These exact rules apply to general Ising spin glass Hamiltonians as in Eq. (1) with *any* bond distribution $P(J)$, discrete or continuous, on arbitrary sparse graphs and lead to fewer but more highly interconnected spins and renormalized bonds (see Ref. 32). Starting from a Hamiltonian as in Eq. (1), in general, new terms are generated by this procedure that have not been part of the Hamiltonian before, such as multispin interactions. Although the number of spins decreases one by one, the number of new terms grows exponentially and the procedure usually becomes inefficient. Yet, near p_c, we can apply a subset of these rules efficiently while leaving the form of the two-spin Hamiltonian in Eq. (1) invariant.

Our recursive set of rules is based on the following observations. Near p_c, most spins have a low degree of interconnectivity; on average, that degree fluctuates around unity in any dimension d. In fact, many spins are entirely disconnected, do not contribute to the Hamiltonian, and can thus be discarded. Degree-1 spins can always be satisfied and are easily traced out, with their bond weight always (at $T=0$) lowering the energy. Once all degree-1 spins have been recursively traced out, any degree-2 spin can be reduced also by replacing it by a new bond between its two neighbors and another offset to the global energy. Having reduced all degree-1 and -2 spins, there is even a "star-triangle" rule to reduce any degree-3 spins while only producing new 2-spin interactions between its neighbors.[31] Although this step could, in principle, create a 3-spin interaction not present in the Hamiltonian in Eq. (1), all such terms involving an odd number of spins vanish due to Z_2 symmetry.

A new rule[32] that proved particularly effective at p_c focuses on spins of arbitrary degree but with "superbonds." A spin x_i has a superbond if one bond's absolute weight dominates, $|J_{i,k}|>\Sigma_{j\neq k}|J_{i,j}|$, all other bonds attached to x_i. In the ground state ($T=0$), that bond is always satisfied and its spin

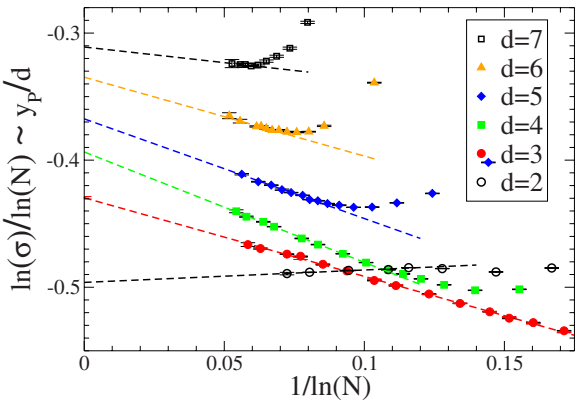

FIG. 2. (Color online) Plot of $\sigma(\Delta E)$ in Eq. (3) as a function of system size $N=L^d$ in extrapolated form. Plotting $\ln(\sigma)/\ln(N)$ vs $1/\ln(N)$ and linearly extrapolating (dashed lines), we extract the asymptotic values for y_P/d in Table I at $1/\ln(N)=0$. Note that the fitted asymptotic regime here corresponds to *orders of magnitude* of scaling in a (less insightful) plot of $\ln\sigma$ vs $\ln N$. Note the increasing corrections to scaling for larger d before asymptotic behavior is obtained.

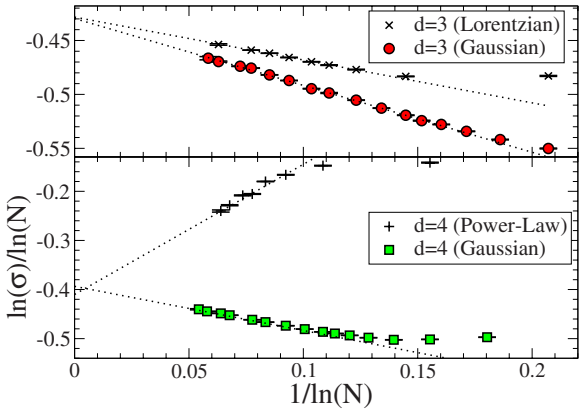

FIG. 3. (Color online) Comparison of the data for $d=3$ (top) and $d=4$ (bottom) for different bond distributions $P(J)$, plotted in the same way as in Fig. 2. There is little difference between the Gaussian and the Lorentzian bonds even in $d=3$, as both are similarly smooth near $J=0$. For our power-law bonds with vanishing support for $|J|<1$, our methods are very inefficient. Yet, at least in $d=4$, those bonds produce results far from but consistent with Gaussian bonds.

determined by its neighbor along that bond. This rule often triggers new avalanches of further reductions with the simpler rules.

Previously, we have applied these rules above p_c to study the defect energy within the spin glass (SG) state (see Fig. 1). Considering dilute lattices with $p>p_c$ but well below $p=1$ allowed the study of larger lattice sizes L for improved scaling and produced results[9,31] in dimensions up to $d=7$, unattainable with undiluted lattices. For $p>p_c$, an optimization heuristic was essential to approximate the ground state of the remainder graph, consisting of highly interconnected spins that remain after all reduction rules have been exhausted. In contrast, at $p=p_c$, these remainder graphs are almost gone entirely. Thus, the attainable system sizes $N=L^d$ are nearly unrestricted and have reached well above $N=10^8$ in our simulations, mostly limited by the need to generate sufficient statistics (i.e., about 10^4 instances for $N=25^6$ or 15^7). Yet, in $d=2$ and 3, the remainder graphs *are* the limiting factors on system sizes (at about $N=10^7$). Although remainders have less than 100 spins, typically well approximated with a good heuristic, we implemented costly exact methods[33] to optimize them. The *slightest* inaccuracy affected the statistical averages, as defect energies ΔE are the difference of two almost equal ground state energies E_0 and E_0'. One technical problem in implementing our algorithm with such large system sizes is posed by memory limitations. Instead of constructing an entire lattice with N spins, each with potentially $2d$ bonds, before applying the reduction rules, we build up the L^d-spin lattice as a sequence of L hyperplanes of L^{d-1} spins. During the process, we keep the first and the most recently added plane fixed but already reduce recursively all spins in the intervening planes as far as possible before the next hyperplane is added. This process requires extensive bookkeeping and backtracking, which can be done fast while reducing memory use by $\sim 1/L$.

In Fig. 2, we present all data of our simulations for $d=2,\ldots,7$ in an extrapolation plot. In Fig. 3, we compare the same data from $d=3$ ($d=4$), together with those from the Lorentzian (power-law) bond distribution $P(J)$, as discussed above. Since our data reach above the upper critical dimension $d_u=6$ (of both percolation and spin glasses) and should approach mean-field behavior, it is most natural to replace L^{y_P} with $N^{y_P/d}$ in Eq. (3) and extrapolate for $y_P/d \sim \ln(\sigma)/\ln(N)$. As Fig. 2 shows, aside from $d=2<d_l$, the extrapolations for $d>d_l$ all seem to share common characteristics and appear to vary smoothly with d. In particular, we have pushed the simulations in $d=7$ to large enough N to conclude that there appears to be no drastic change in the scaling behavior above d_u. Increasing corrections make it harder to reach asymptotic scaling beyond $d=7$. Interestingly, all transients in Fig. 2 themselves extrapolate to an intercept consistent with $-1/2$, indicative of a higher-order correction term with a d-independent exponent.

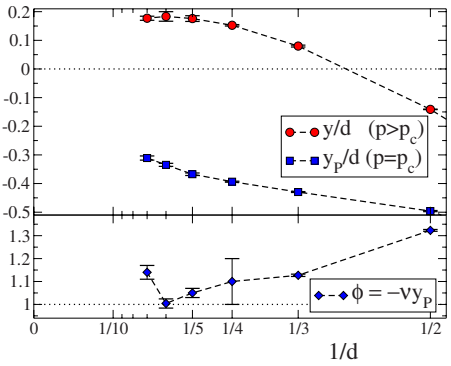

FIG. 4. (Color online) Plot of the exponents y_P/d (top) and phi (bottom) in Table I as a function of $1/d$. For comparison, also plotted (top) are the stiffness exponents y/d inside the spin-glass regime (Ref. 9) ($p>p_c$). Some of the large error bars for $\phi=-\nu y_P$ originate with uncertainties in ν (Ref. 11).

The result in $d=2$, where $T_g=0$, is very close to that theoretically predicted in Ref. 10, $y_P \approx -0.99$, and could conceivably be $=-1$ exactly, as it is in $d=1$ (where $p_c=1$). That would suggest that the spin glass on a $d=2$ percolation cluster essentially consists of a spanning linear backbone of bonds.

In Fig. 4, we plotted y_P/d and ϕ from Table I vs $1/d$ to explore the large-d limit. This extrapolation plot suggests a trend toward a vanishing value for y_P/d at $1/d=0$; i.e., y_P varies sublinearly with d. In comparison, the data for the stiffness exponents y/d inside the spin-glass regime replotted from Ref. 9 appear consistent with the prediction[34,35] of $y/d \sim 1/6$. It would be difficult to suspect a systematic bias in the apparent drift of the high-d data points for y_P/d, as the computations are exact. Yet, statistical errors clearly become increasingly significant for larger d (see Fig. 2). It is not obvious how to directly obtain y_P for $d=\infty$, which may correspond to a (replica-symmetric) $T=T_g=0$ Viana–Bray model[36] at the Erdös-Rényi percolation point. [Such a calculation has been undertaken for the fully connected (replica-symmetry broken, $T<T_g$) SK model.[37]] Finally, we note a distinct minimum in ϕ, with $\phi_6 \approx 1$, exactly at the upper critical dimension $d_u=6$ due to the product of increasing $|y_P|$ and decreasing ν.

This work has been supported by Grant No. 0312510 from the Division of Materials Research at the NSF and by the Emory University Research Council. We thank S. Mertens for providing computer time at Magdeburg University and P. Nordblat for helpful discussions.

[1] *Spin Glasses and Random Fields*, edited by A. P. Young (World Scientific, Singapore, 1998).
[2] G. Parisi, arXiv:0711.0369 (unpublished).
[3] K. H. Fischer and J. A. Hertz, *Spin Glasses* (Cambridge University Press, Cambridge, 1991).
[4] *New Optimization Algorithms in Physics*, edited by A. Hartmann and H. Rieger (Springer, Berlin, 2004).
[5] K. Binder and A. P. Young, Rev. Mod. Phys. **58**, 801 (1986).
[6] S. Boettcher, Eur. Phys. J. B **38**, 83 (2004).
[7] B. W. Southern and A. P. Young, J. Phys. C **10**, 2179 (1977).
[8] A. J. Bray and M. A. Moore, J. Phys. C **17**, L463 (1984).
[9] S. Boettcher, Phys. Rev. Lett. **95**, 197205 (2005).
[10] J. R. Banavar, A. J. Bray, and S. Feng, Phys. Rev. Lett. **58**, 1463 (1987).
[11] B. D. Hughes, *Random Walks and Random Environments* (Oxford University Press, Oxford, 1996).
[12] D. Stauffer and A. Aharony, *Introduction to Percolation Theory*, 2nd ed. (CRC, Boca Raton, FL, 1994).
[13] Y. Deng and H. W. J. Blöte, Phys. Rev. E **72**, 016126 (2005).
[14] C. D. Lorenz and R. M. Ziff, Phys. Rev. E **57**, 230 (1998).
[15] P. Grassberger, Phys. Rev. E **67**, 036101 (2003).
[16] M. J. Stephen and G. S. Grest, Phys. Rev. Lett. **38**, 567 (1977).
[17] M. R. Giri and M. J. Stephen, J. Phys. C **11**, L541 (1978).
[18] B. W. Southern, A. P. Young, and P. Pfeuty, J. Phys. C **12**, 683 (1979).
[19] A. Coniglio, Phys. Rev. Lett. **46**, 250 (1981).
[20] M. Aizenman, J. T. Chayes, L. Chayes, and C. M. Newman, J. Phys. A **20**, L313 (1987).
[21] S. Shapira, L. Klein, J. Adler, A. Aharony, and A. B. Harris, Phys. Rev. B **49**, 8830 (1994).
[22] G. Munninghoff, E. Hellner, W. Treutmann, N. Lehner, and G. Heger, J. Phys. C **17**, 1281 (1984).
[23] T. Vojta and J. A. Hoyos, arXiv:0707.0658 (unpublished).
[24] S. J. Poon and J. Durand, Phys. Rev. B **18**, 6253 (1978).
[25] O. Beckman, E. Figueroa, K. Gramm, L. Lundgren, K. V. Rao, and H. S. Chen, Phys. Scr. **25**, 726 (1982).
[26] E. Vincent, in *Ageing and the Glass Transition*, Springer Lecture Notes in Physics Vol. 716, edited by M. Henkel, M. Pleimling, and R. Sanctuary (Springer, Heidelberg, 2007).
[27] H. G. Katzgraber, M. Körner, and A. P. Young, Phys. Rev. B **73**, 224432 (2006).
[28] K. Matho, J. Low Temp. Phys. **35**, 165 (1979).
[29] A. J. Bray and S. Feng, Phys. Rev. B **36**, 8456 (1987).
[30] S. Boettcher, Eur. Phys. J. B **33**, 439 (2003).
[31] S. Boettcher, Europhys. Lett. **67**, 453 (2004).
[32] S. Boettcher and J. Davidheiser, arXiv:0802.1941 (unpublished).
[33] T. Klotz and S. Kobe, J. Phys. A **27**, L95 (1994).
[34] G. Parisi and T. Rizzo, arXiv:0706.1180 (unpublished).
[35] T. Aspelmeier, A. Billoire, E. Marinari, and M. A. Moore, arXiv:0711.3445.
[36] L. Viana and A. J. Bray, J. Phys. C **18**, 3037 (1985).
[37] T. Aspelmeier, M. A. Moore, and A. P. Young, Phys. Rev. Lett. **90**, 127202 (2003).